International Journal of Solids and Structures 51 (2014) 4215–4220

Contents lists available at ScienceDirect

International Journal of Solids and Structures

journal homepage: www.elsevier.com/locate/ijsolstr

Rapid simulation procedure for fretting wear on the basis of the method of dimensionality reduction

A.V. Dimaki [a], A.I. Dmitriev [a,d], Y.S. Chai [b], V.L. Popov [c,d,e,*]

[a] Institute of Strength Physics and Material Science, Russian Academy of Science, Tomsk, Russia
[b] Yeungnam University, School of Mechanical Engineering, Gyeongsan 712-749, South Korea
[c] Berlin University of Technology, Berlin, Germany
[d] Tomsk State University, 634050 Tomsk, Russia
[e] Tomsk Polytechnic University, 634036 Tomsk, Russia

ARTICLE INFO

Article history:
Received 7 December 2013
Received in revised form 3 June 2014
Available online 15 August 2014

Keywords:
Fretting wear
Method of dimensionality reduction
Numerical simulation

ABSTRACT

We suggest a numerical procedure for rapid simulation of fretting wear in a contact of two bodies subjected to tangential oscillations with a small amplitude. The incremental wear in each point of contact area is calculated using the Reye–Archard–Khrushchov wear criterion. For applying this criterion, the distributions of pressure and relative displacements of bodies are required. These are calculated using the method of dimensionality reduction (MDR).

1. Introduction

Fretting wear occurs if two bodies are pressed against each other and are subsequently subjected to oscillations with small amplitude. Even if there is no gross slip in the contact, tangential slip occurs at the border of the contact area leading to wear and fatigue. Fretting wear was in the past an object of intensive experimental investigation and theoretical simulation for such applications as fretting of tubes in steam generators and heat exchangers (Ko, 1979; Fisher et al., 1995; Lee et al., 2009), joints in orthopedics (Collier, 1992), electrical connectors (Antler, 1985), and dovetail blade roots of gas turbines (Rajasekaran and Nowell, 2006; Ciavarella and Demelio, 2001) as well as many others. Most theoretical works were concerned with finite element (Ding et al., 2009; Mohd Tobia et al., 2009) or boundary element simulations (Lee et al., 2009). Thus in (Ding et al., 2007) a fretting wear modelling of complex geometries like spline coupling with finite element modeling was considered. Even while these simulations provided a complete picture of fretting wear, they still require too much computational time to be implemented as an interface in larger dynamic simulations. In a conventional finite element fretting simulation most of the time is wasted not for the calculation of wear itself but for the solution of the normal and tangential contact problems of progressively changing profile. That is why there are a lot of alternative approaches to a full finite element analysis. Examples of analytical and semi-analytical approaches were given in Nowell (2010) and Hills et al. (2009). In the present paper, we suggest to do this step using the method of dimensionality reduction (Heß, 2012; Popov, 2013; Popov and Heß, 2013; Popov, 2012). This drastically reduces the time of the whole simulation.

2. The method of dimensionality reduction

In this section we quickly recapitulate the main rules of the method of dimensionality reduction (Heß, 2012; Popov and Heß, 2013, 2014a). We consider a contact of a three-dimensional rotationally symmetric profile $z = I(r)$ and an elastic half-space. The profile is first transformed into a one-dimensional profile $g(x)$ according to the MDR-rule (Heß, 2012; Popov and Heß, 2013)

$$g(x) = |x| \int_0^{|x|} \frac{I'(r)dr}{\sqrt{x^2 - r^2}} \tag{1}$$

as illustrated in Fig. 1, where $I'(r)$ is a first derivative of $I(r)$.

The reverse transformation is given by the integral

$$I(r) = \frac{2}{\pi} \int_0^r \frac{g(x)}{\sqrt{r^2 - x^2}} dx \tag{2}$$

The profile (1) is pressed to a given indentation depth d into an elastic foundation consisting of independent springs with spacing

* Corresponding author at: Berlin University of Technology, Berlin, Germany.
E-mail address: v.popov@tu-berlin.de (V.L. Popov).

http://dx.doi.org/10.1016/j.ijsolstr.2014.08.003
0020-7683/

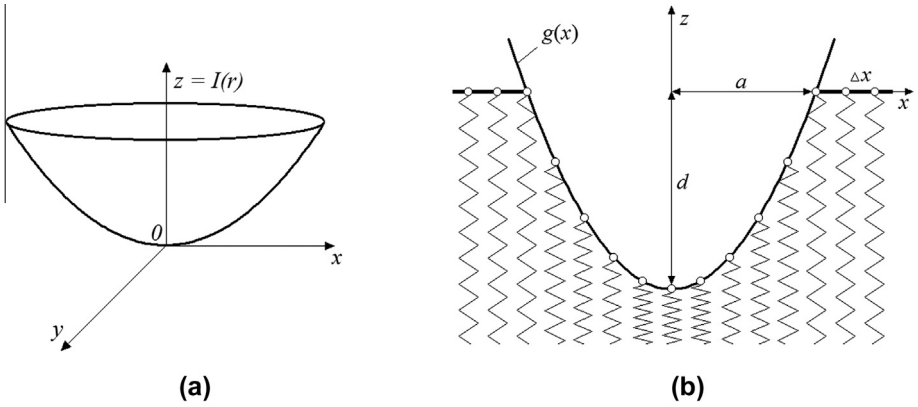

Fig. 1. The 3-dimensional body of revolution (a); and the corresponding one-dimensional MDR-transformed profile in a contact with the elastic foundation.

Δx (Fig. 1b) whose normal and tangential stiffness is given by (Popov and Heß, 2013)

$$\begin{aligned} k_z &= E^*\Delta x \\ k_x &= G^*\Delta x \end{aligned}, \tag{3}$$

where E^* is the effective elastic modulus

$$\frac{1}{E^*} = \frac{1-\nu_1^2}{E_1} + \frac{1-\nu_2^2}{E_2} \tag{4}$$

and G^* the effective shear modulus

$$\frac{1}{G^*} = \frac{(2-\nu_1)}{4G_1} + \frac{(2-\nu_2)}{4G_2}, \tag{5}$$

E_1 and E_2 are the Young's moduli, G_1 and G_2 the shear moduli of the indenter and the half -space, and ν_1 and ν_2 are their Poisson-ratios. Note that throughout this paper, we assume that the contacting materials satisfy the condition of "elastic similarity"

$$\frac{1-2\nu_1}{G_1} = \frac{1-2\nu_2}{G_2} \tag{6}$$

that guarantees the decoupling of the normal and tangential contact problems (Johnson, 1985). Note that the choice of the spatial step Δx is arbitrary as long as it is much smaller than all characteristic length scales of the problem; the solution does not depend on its choice.

The vertical displacement of an individual spring is given by

$$u_z(x) = d - g(x) \tag{7}$$

and the resulting normal force is given by

$$f_z(x) = E^*\Delta x(d - g(x)). \tag{8}$$

The linear force density is therefore

$$q_z(x) = \frac{f_z(x)}{\Delta x} = E^* u_z(x) = E^*(d - g(x)). \tag{9}$$

The contact radius a is determined by the condition

$$g(a) = d. \tag{10}$$

The total normal force is obtained by integration over all springs in contact:

$$F_N = 2E^* \int_0^a (d - g(x))\mathrm{d}x. \tag{11}$$

According to the MDR rules, the distribution of normal pressure p in the initial three-dimensional problem can be calculated using the following integral transformation (Heß, 2012; Popov and Heß, 2013):

$$p(r) = -\frac{1}{\pi}\int_r^\infty \frac{q_z'(x)}{\sqrt{x^2 - r^2}}\mathrm{d}x = \frac{E^*}{\pi}\int_r^a \frac{g'(x)}{\sqrt{x^2 - r^2}}\mathrm{d}x. \tag{12}$$

Note that all above results obtained by the MDR, represent *exact* solutions of the corresponding three-dimensional problem. As was shown by Galin (1961), the transformation (1) maps the complete three-dimensional contact problem to a one-dimensional contact with an elastic foundation. All three-dimensional properties (as displacements, stresses and so on) can be obtained for the solution of the linear elastic foundation problem by appropriate integral transformations. This solution is *exact* and was used later in the well-known publication by Sneddon (1965). This solution can be generalized to all contact problems which can be reduced to the normal contact problem.

The complete proof for tangential contact can be found in the book (Popov and Heß, 2014b).

If the indenter is now moved in the tangential direction by $u_x^{(0)}$, the springs in contact will first stick to the indenter thus producing tangential force $f_x = k_x u_x^{(0)}$ until this force achieves the critical value μf_z, where μ is the coefficient of friction. After this, the tangential force remains constant and equal to μf_z while the springs begin to slide. The same is valid if the movement starts from an arbitrary stress state of a spring. It either follows the indenter, if the tangential force is smaller than the critical one or it slides, in which case the tangential force is equal to the critical value. Thus, for any incremental change of the tangential displacement the following equations are valid:

$$\begin{aligned} \Delta u_x(x) &= \Delta u_x^{(0)}, \quad \text{if} |k_x u_x(x)| < \mu f_z \\ u_x(x) &= \pm\tfrac{\mu f_z(x)}{k_x}, \quad \text{in the sliding state} \end{aligned}. \tag{13}$$

The sign in the last line of this equation depends on the direction of movement of the indenter. By following incremental changes in the indenter position, the absolute tangential displacement can be determined unambiguously at any location and any point in time. Therefore, the tangential force will also be determined:

$$f_x = k_x u_x(x) = G^*\Delta x \cdot u_x(x). \tag{14}$$

The tangential force density is equal to

$$q_x(x) = \frac{f_x}{\Delta x} = G^* u_x(x). \tag{15}$$

Distributions of tangential stresses $\tau(r)$ and displacements $u_x^{(3D)}(r)$ in the initial three-dimensional problem are defined by equations similar to (2) and (12), (Popov and Heß, 2014b):

$$u_x^{(3D)}(r) = \frac{2}{\pi}\int_0^r \frac{u_x(x)dx}{\sqrt{r^2 - x^2}}, \tag{16}$$

$$\tau(r) = -\frac{1}{\pi}\int_r^\infty \frac{q_x'(x)dx}{\sqrt{x^2 - r^2}} = -\frac{G^*}{\pi}\int_r^\infty \frac{u_x'(x)dx}{\sqrt{x^2 - r^2}}. \tag{17}$$

As it was shown by Cattaneo (1938) and Mindlin (1949) the tangential contact with Coulomb friction is equivalent to a superposition of normal contacts. This allows one to apply the MDR to tangential contacts, whereby the Coulomb law in the one-dimensional image is applied not to stresses but to spring forces. The exact formal proof of this procedure can be found in Popov and Heß (2014b, Chapter 18).

Note, that all transformations used in the MDR have an integrable singularity in the definition region. As theoretically predicted in Hills et al. (2009), the normal and shear stresses will have the same type of singularities near the edge of the worn region of indenter. However, due to integrability, this type of singularity does not pose a serious problem for numerical implementation of the method. In the developed numerical procedure we apply the regularized algorithm of calculation of $p(r)$ and $\tau(r)$ that correctly treats the singularities to avoid instabilities and non-physical oscillations of the profile of indenter. In numerical procedure, singularities of $p(r)$ and $\tau(r)$ transform to relatively high peaks (seen in Fig. 2c and Fig. 2d).

3. Calculation of wear

In this paper, we assume for simplicity that both bodies in contact are elastic but only one of them, the indenter, is subjected to wear. We apply the simplest and most broadly used wear equation stating that the wear volume is proportional to the dissipated energy and inversely proportional to the hardness σ_0 of the worn material. This kind of wear criterion was first proposed by Reye (1860) and later justified in detail theoretically and experimentally by for abrasive wear (Khrushchov and Babichev, 1960) and for adhesive wear (Archard and Hirst, 1956). The local formulation of this criterion means that the linear change of the three-dimensional profile is given by the equation

$$\Delta I(r) = \frac{k_{wear}}{\sigma_0}\tau(r)\left(\Delta u_x^{(3D)}(r) - \Delta u_x^{(0)}\right), \tag{18}$$

where k_{wear} is the dimensionless wear coefficient and symbol Δ means the increment of corresponding parameter. No wear occurs in positions where either the tangential stress or the relative displacement is zero.

The simulation procedure consists of three repeating steps:

1. Using the current three-dimensional profile, the MDR-transformed one-dimensional profile is calculated using Eq. (1).
2. The tangential contact problem is solved using Eqs. (10), (11), (13), (16), (17).
3. The change of the three-dimensional profile is calculated according to (18).

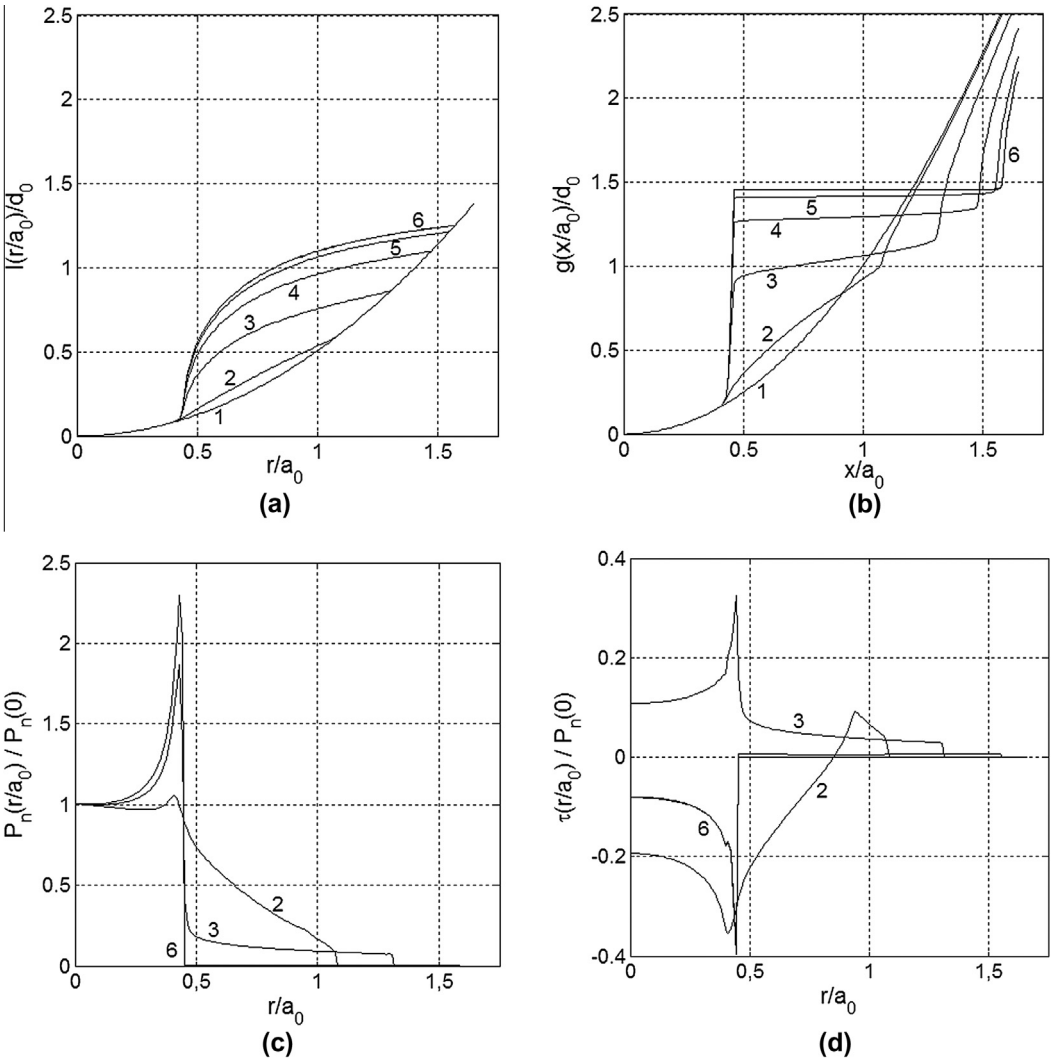

Fig. 2. (a) Development of the shape of an initially parabolic profile due to fretting wear. The curve "1" shows the initial profile, further curves correspond to the following normalized number of oscillation cycles: (2) $\tilde{N} = 0.04$; (3) $\tilde{N} = 0.16$; (4) $\tilde{N} = 0.36$; (5) $\tilde{N} = 0.64$; (6) $\tilde{N} = 1$. (b) Development of the corresponding MDR-transformed profiles. (c) and (d) Development of normal pressure $p(r/a_0)$ and tangential stress $\tau(r/a_0)$. Both quantities are normalized by $p(0)$.

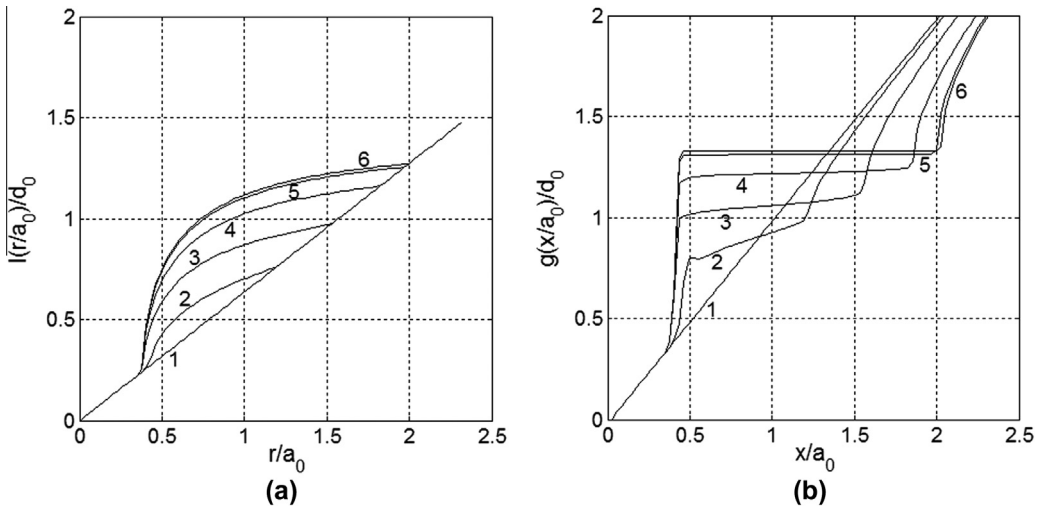

Fig. 3. (a) Development of the shape of an initially conical profile due to fretting wear. The curve "1" shows the initial profile, further curves correspond to the following normalized number of oscillation cycles: (2) $\tilde{N} = 0.1$; (3) $\tilde{N} = 0.4$; (4) $\tilde{N} = 0.9$; (5) $\tilde{N} = 1.6$; (6) $\tilde{N} = 2.5$. (b) Development of the corresponding MDR-transformed profiles.

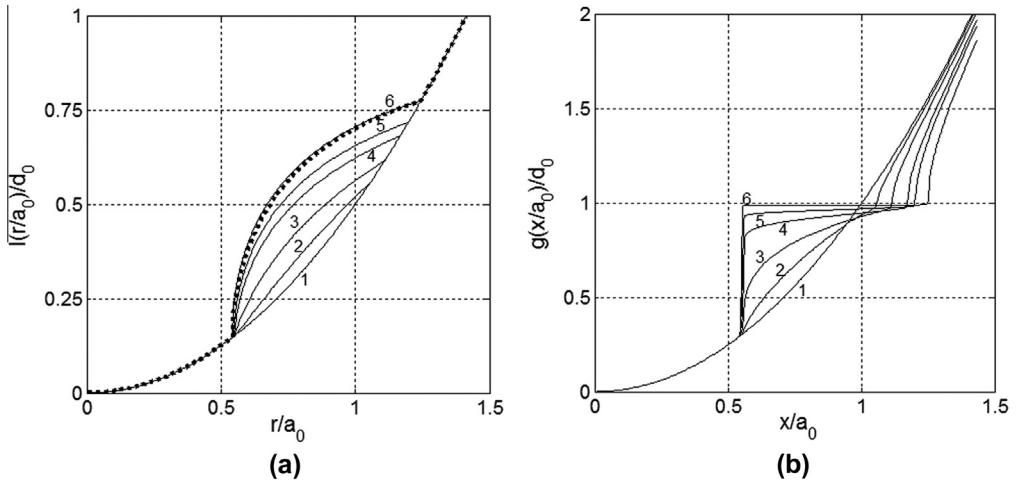

Fig. 4. (a) Development of the shape of an initially parabolic profile under the constant indentation depth. The curve "1" shows the initial profile, further curves correspond to the following normalized number of oscillation cycles: (2) $\tilde{N} = 0.16$; (3) $\tilde{N} = 0.36$; (4) $\tilde{N} = 0.64$; (5) $\tilde{N} = 1.0$; (6) $\tilde{N} = 9$. Dotted line shows the analytical estimate of worn profile of indenter at "shakedown" state. (b) Development of the corresponding MDR-transformed profiles.

In each step one gets the real three-dimensional profile, its one-dimensional MDR-image as well as distributions of normal and tangential stresses.

Let us denote the indentation depth of the *initial* profile with d_0 and the corresponding initial contact radius with a_0. All vertical coordinates will be normalized by d_0 and the horizontal coordinates by a_0. Thus, we will use the following dimensionless variables:

$$\begin{aligned} \tilde{I} &= I/d_0, \quad \tilde{d} = d/d_0 \\ \tilde{r} &= r/a_0, \quad \tilde{x} = x/a_0 \end{aligned}. \tag{19}$$

If the indenter oscillates with an amplitude $U^{(0)}$, then the characteristic wear volume during one cycle of oscillation will have the order of magnitude of $\Delta I \approx \frac{k}{\sigma_0}\frac{\mu F_N}{\pi a_0^2}U^{(0)}$; the wear depth of the indenter will reach the order of magnitude of d_0 in a number of cycles

$$N_0 = \frac{d_0}{\Delta I} \approx \frac{\pi a_0^2 d_0 \sigma_0}{k\mu F_N U^{(0)}}. \tag{20}$$

The actual number of cycles will be normalized to this characteristic value:

$$\tilde{N} = \frac{N}{N_0}. \tag{21}$$

For oscillation amplitudes smaller than μd, the contact area will be divided into stick and slip areas (Cattaneo, 1938; Mindlin, 1949; Jäger, 1995; Ciavarella and Hills, 1999). Let us denote the radius of the stick region by c. Wear will occur only outside this region. In the absence of gross slip in the whole contact area this will always lead to a "shakedown" state with no further wear (Ciavarella and Hills, 1999; Popov, 2014).

4. Simulation examples

In this section, we present simulation results obtained with the above algorithm for the cases of parabolic and conical profiles as well as for the initially worn parabolic indenter.

4.1. Parabolic indenter

The initial profile is in this case $I_0(r) = r^2/(2R)$, where R is the radius of curvature; the corresponding one-dimensional MDR-image

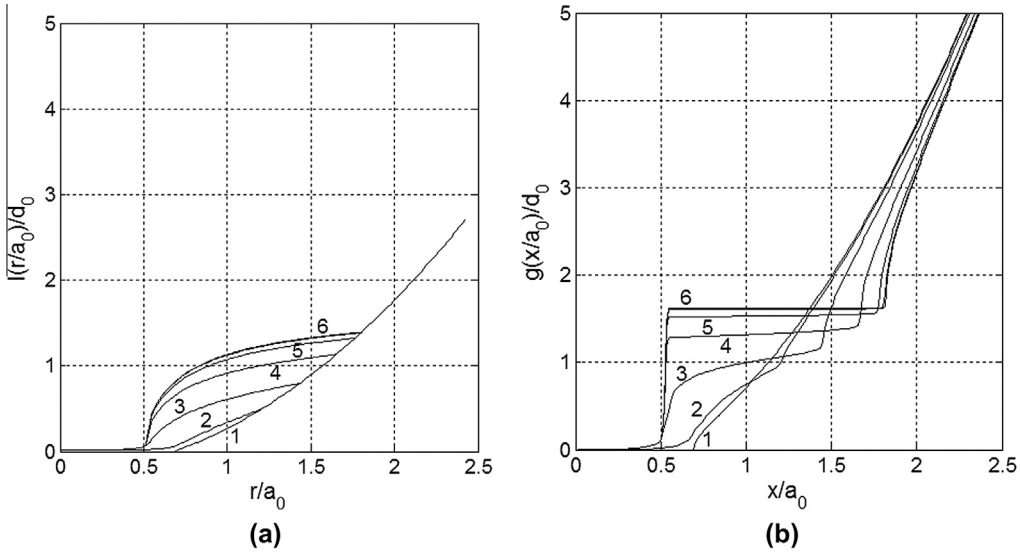

Fig. 5. (a) Development of the shape of an initially parabolic indenter with initial wear (blunted tip) due to fretting wear. The curve "1" shows the initial profile, further curves correspond to the following normalized number of oscillation cycles: (2) $\tilde{N} = 0.04$; (3) $\tilde{N} = 0.16$; (4) $\tilde{N} = 0.36$; (5) $\tilde{N} = 0.64$; (6) $\tilde{N} = 1.44$. (b) Development of the corresponding MDR-transformed profiles.

is $g_0(r) = x^2/R$. The initial radius of contact is $a_0 = \sqrt{d_0 R}$. The amplitude of the tangential oscillation was chosen in such a way that the radius of the initial stick region was $c = 0.4a_0$. The development of the profile of the indenter due to wear with increasing number of cycles is shown in Fig. 2.

4.2. Conical indenter

The initial profile is in this case $I_0(r) = r\tan\theta$, and the corresponding one-dimensional MDR-image is $g_0(r) = \frac{\pi}{2}|x|\tan\theta$. The initial contact radius is given by $a_0 = \frac{2}{\pi}\frac{d_0}{\tan\theta}$. The amplitude of the tangential oscillation was chosen in such a way that the radius of the initial stick region was $c = 0.4a_0$. The development of the profile of the indenter due to wear with increasing number of cycles is shown in Fig. 3.

4.3. Parabolic indenter with constant indentation depth

In order to compare the numerical results of our model with the exact analytic solution provided in Popov (2014), we considered also the case where the oscillations are applied under conditions of the given indentation depth d. We hold an indentation depth constant during the whole calculation. The initial profile is again $I_0(r) = r^2/(2R)$, where R is the radius of curvature; the corresponding one-dimensional MDR-image is $g_0(r) = x^2/R$. The initial radius of contact is $a_0 = \sqrt{d_0 R}$. The amplitude of the tangential oscillation was chosen in such a way that the radius of the initial stick region was $c = 0.4a_0$. The development of the profile of the indenter due to wear with increasing number of cycles is shown in Fig. 4.

One can see an excellent coincidence of the analytical solution of the profile of indenter in "shakedown" state and the profile, obtained numerically in our model (Fig. 4a, curve 6).

4.4. Parabolic indenter with initial wear

Simulation of the fretting of initially worn parts is the problem of practical importance. We demonstrate how the method works in this case, we considered the wear process of a parabolic indenter with initially worn (blunted) tip (see Fig. 5a). Moreover, the MDR allows simulation of wear of a body of revolution with an arbitrary profile.

Compared with finite element simulation, the proposed algorithm is extremely fast: in the examples above approximately 10^4 cycles were simulated (almost up to the final shakedown state) and took only 20 s each on a standard PC. The time step in our simulations was selected from the conditions of stability and immutability of the algorithm results in a further decrease in the time step. This selection procedure of allowable time step was performed for each calculation. The choice of the spacing between the springs, Δx, was done according to the theorem of Wiener (1930), stating that the value of the spatial step $\Delta x_{\max}$ for a task is defined by the minimum spatial wavelength λ_{min} in the spectral density of the surface profile and is equal to $\Delta x_{max} = \lambda_{min}/2$. So, the spatial step Δx in the task is defined as $\Delta x <= \lambda_{min}/2$.

It is interesting to note that the development of the one-dimensional MDR-images appears to be simpler than the development of the original three-dimensional worn profile. This suggests a possibility of an (at least approximate) wear formulation directly in the space of MDR-images. If this would be possible, this would accelerate the calculation further by several orders of magnitude. An attempt of such formulation is done in the paper (Li et al., 2014).

5. Conclusions

We have studied the problem of wear of a rotationally symmetric profile subjected to oscillations with small amplitude. It is well known that small oscillations lead to the appearance of a sliding region at the border of the contact area while the inner parts of the contact area may still stick. Both the sliding configuration and the wear intensity remain rotationally isotropic during the whole wear process. This allows solving the corresponding normal and tangential problems exactly using the method of dimensionality reduction which replaces the three-dimensional contact problem with a contact problem with an elastic foundation. This drastically reduces the simulation time compared with conventional finite element simulations. At this time, the described method is only applicable to rotationally symmetric profiles, but we are working on its extension to contact with elliptic contact areas.

Acknowledgment

The authors acknowledge many valuable discussions with M. Heß, M. Ciavarella, A. Filippov, and M. Popov. This work was partially supported by Deutsche Forschungsgemeinschaft (DFG), Deutscher Akademischer Austausch Dienst (DAAD), Russian Science Foundation (RSF) grant No. 14-19-00718, and the Ministry of Education of the Russian Federation.

References

Antler, M., 1985. Survey of contact fretting in electrical connectors. Compon. Hybrids Manuf. Technol. 8, 87–104.
Archard, J.F., Hirst, W., 1956. The wear of metals under unlubricated conditions. Proc. R. Soc. Lond. A 236, 397–410. http://dx.doi.org/10.1098/rspa.1956.0144.
Cattaneo, C., 1938. Sul contatto di due corpi elastici: distribuzione locale degli sforzi. Rend. dell'Accad. Naz. dei Lincei. 27, 342–348, 434–436, 474–478.
Ciavarella, M., Demelio, G., 2001. A review of analytical aspects of fretting fatigue, with extension to damage parameters, and application to dovetail joints. Int. J. Solids Struct. 38, 1791–1811.
Ciavarella, M., Hills, D.A., 1999. Brief note: some observations on the oscillating tangential forces and wear in general plane contacts. Eur. J. Mech. A. Solids 18, 491–497.
Collier, J.P. et al., 1992. Mechanisms of failure of modular prostheses. Clin. Orthpaedics Relat. Res., 129–139.
Ding, J., McColl, I.R., Leen, S.B., 2007. The application of fretting wear modelling to a spline coupling. Wear 262, 1205–1216.
Ding, J., Bandak, G., Leen, S.B., et al., 2009. Experimental characterization and numerical simulation of contact evolution effect on fretting crack nucleation for Ti-6Al-4V. Tribol. Int. 42, 1651–1662.
Fisher, N.J., Chow, A.B., Weckwerth, M.K., 1995. Experimental fretting wear studies of steam generator materials. J. Press. Vessel Technol. 117, 312–320.
Galin, L.A., 1961. Contact Problems in the Theory of Elasticity. North Carolina State College, USA.
Heß, M., 2012. On the reduction method of dimensionality: the exact mapping of axisymmetric contact problems with and without adhesion. Phys. Mesomech. 15, 264–269.
Hills, D.A., Sackfield, A., Paynter, R.J.H., 2009. Simulation of fretting wear in half-plane geometries: Part I – the solution for long term wear. J. Tribol. 131, 031401.
Jäger, J., 1995. Axi-symmetric bodies of equal material in contact under torsion or shift. Arch. Appl. Mech. 65, 478–487.
Johnson, K.L., 1985. Contact Mechanics. Cambridge University Press.
Khrushchov, M.M., Babichev, M.A., 1960. Investigation of wear of metals (Исследованиеизнашиванияметаллов). Russian Academy of Sciences, Moscow.
Ko, P.L., 1979. Experimental studies of tube frettings in steam generators and heat exchangers. J. Press. Vessel Technol. 101, 125–133.
Lee, C.Y., Tian, L.S., Bae, J.W., Chai, Y.S., 2009. Application of influence function method on the fretting wear of tube-to-plate contact. Tribol. Int. 42, 951–957.
Li, Q., Filippov, A.E., Dimaki, A.V., Chai, Y.S., Popov, V.L., 2014. Simplified simulation of fretting wear using the method of dimensionality reduction. Phys. Mesomech. 17, 236–241.
Mindlin, R.D., 1949. Compliance of elastic bodies in contact. J. Appl. Mech. 16, 259–268.
Mohd Tobia, A.L., Dinga, J., Bandaka, G., Leenb, S.B., Shipwaya, P.H., 2009. A study on the interaction between fretting wear and cyclic plasticity for Ti–6Al–4V. Wear 267, 270–282.
Nowell, D., 2010. Simulation of fretting wear in half-plane geometries – Part II: analysis of the transient wear problem using quadratic programming. J. Tribol. 132, 021402.
Popov, V.L., 2012. Basic ideas and applications of the method of reduction of dimensionality in contact mechanics. Phys. Mesomech. 15, 254–263.
Popov, V.L., 2013. Method of reduction of dimensionality in contact and friction mechanics: a linkage between micro and macro scales. Friction 1, 41–62.
Popov, V.L., 2014. Analytic solution for the limiting shape of profiles due to fretting wear. Sci. Rep. 4, 3749. http://dx.doi.org/10.1038/srep03749.
Popov, V.L., Heß, M., 2013. Methode der Dimensionsreduktion in Kontaktmechanik und Reibung. Springer.
Popov, V.L., Heß, M., 2014a. Method of dimensionality reduction in contact mechanics and friction: a users handbook. I. Axially-symmetric contacts. Facta Universitatis, series Mech. Eng. 12 (1), 1–14.
Popov, V.L., Heß, M., 2014b. Method of Dimensionality Reductions in Contact Mechanics and Friction. Springer.
Rajasekaran, R., Nowell, D., 2006. Fretting fatigue in dovetail blade roots: experiment and analysis. Tribol. Int. 39, 1277–1285.
Reye, T., 1860. Zur Theorie der Zapfenreibung. Der Civilingenieur 4, 235–255.
Sneddon, I.N., 1965. The relation between load and penetration in the axisymmetric Boussinesq problem for a punch of arbitrary profile. Int. J. Eng. Sci. 3 (1), 47–57.
Wiener, N., 1930. Generalized Harmonic Analysis. Acta Math. 55, 117–258.